View metadata, citation and similar papers at core.ac.uk

brought to you by CORE

Analysis of SDFT based phase detection system for grid synchronization of distributed generation systems

B. Chitti Babu [a, *], K. Sridharan [b], Eugeniusz Rosolowski [a], Zbigniew Leonowicz [a]

[a] Institute of Electrical Power Engineering, Wroclaw University of Technology, Poland
[b] Department of Electrical & Electronics Engineering, SAVEETHA University, Chennai, India

A fast and exact detection of phase and fundamental frequency of grid voltage/current is essential for calculating accurate reference signal in order to implement the control algorithm of inverter-interfaced distributed generation (DG) system and realize precise harmonic compensation. However, the methods adapted in the literature based on phase locked loop (PLL) exhibits large phase error, be difficult to implement, and their performance is also indistinct under conditions where the grid frequency varies or the supply is distorted with low frequency harmonics. This paper explores an improved phase detection system for DG system based on Sliding Discrete Fourier Transform (SDFT). The proposed SDFT based phase detection shows a robust phase tracking capability with fast transient response under adverse situation of the grid. Moreover, SDFT phase detection system is more efficient as it requires small number of operations to extract a single frequency component, thereby reducing computational complexity and simpler than DFT. The superior performance of proposed SDFT phase detection system is analyzed and the obtained results are compared with Discrete Fourier Transform (DFT) filtering to confirm the feasibility of the study under different grid environment such as high frequency harmonic injection, frequency deviation, and phase variation etc.

d.

1. Introduction

As the renewable energy sources are intermittent in nature, in order to ensure safe and reliable operation of power system based on new and renewable sources at par with conventional power plants, usually power system operators should satisfy the grid code requirements such as grid stability, fault ride through, power quality improvement, grid synchronization and active/reactive power control etc [1]. Grid code requirements are generally ach- ieved by grid-side converter based on power electronic devices. According to grid code requirements, operation capacity of grid- side converter (GSC) largely depends on the information about the phase of the grid voltage, and the control system must be capable of tracking the phase angle of grid voltage/current accurately.

estimation [5]. However the method based on FIR Filtering, can also be complex to understand and implement. A new adaptive notch filtering based phase detection system is proposed in Yazdani et al. for single-phase system and it shows that the proposed system is simple, robust and less complexity in digital implementation [6]. However, transient response is sluggish especially during grid voltage/frequency variation. Brendan Peter McGrath et al., have proposed new recursive DFT filter for phase error correction for line synchronization by using time window and phase error correction method [7]. However it is found that, the recursive DFT filter produce large steady state error due to variable sample rate. P. Sumathi. et al. has introduced SDFT filtering for extracting the fundamental real and imaginary signals from the harmonic-rich periodic input signal. However, the stability problem arises due to band pass characteristics of SDFT filtering.

This paper presents an improved phase detection system for grid-interactive power converter based on Sliding Discrete Fourier Transform (SDFT). The proposed SDFT based phase detection shows a robust phase tracking capability with fast transient response under adverse situation of grid. Moreover, SDFT phase detection system is more efficient as it requires small number of operations to extract a single frequency component, thereby reducing computational complexity and simpler than DFT. The immediate advantages of the proposed sliding DFT PLL are: frequency adaptability, full account of unbalanced conditions, high degree of immunity to disturbances and harmonics, and structural robustness. The superior performance of proposed SDFT phase detection system is studied and the obtained results are compared with DFT filtering to confirm the feasibility of the study under different grid environment such as high harmonic injection, frequency deviation, and phase variation etc.

2. Phase detection by Synchronous Reference Frame (SRF) PLL

Synchronous Reference Frame (SRF) PLL is mainly used for tracking the phase angle in case of 3-phase signals which uses Park's Transformation of a 3-phase signal as the phase-detector (PD). The schematic diagram of three-phase SRF PLL is illustrated in Fig. 1 [9]. To obtain the phase information, the three phase (V_a, V_b, V_c) grid voltages are transformed into two phases (V_α, V_β) in stationary reference frame ($\alpha - \beta$) by using Clark's transformation and these two phases are further transformed into direct and quadrature (V_d, V_q) axis components in synchronously rotating reference frame (d – q) by using Park transformation. Then the phase angle θ is tracked by synchronously rotating voltage space vector along q or d axis by using PI controller. The grid voltage is given as

$$V_a = V_m \sin\theta \tag{1}$$

$$V_b = V_m \sin\left(\theta - \frac{2\pi}{3}\right) \tag{2}$$

$$V_c = V_m \sin\left(\theta + \frac{2\pi}{3}\right) \tag{3}$$

where 'θ' is the estimated phase angle. The $\alpha\beta$-transformation matrix is given as

$$T_{\alpha\beta} = \frac{2}{3}\begin{bmatrix} 1 & -\frac{1}{2} & -\frac{1}{2} \\ 0 & \frac{\sqrt{3}}{2} & -\frac{\sqrt{3}}{2} \end{bmatrix} \tag{4}$$

$$V_{\alpha\beta} = T_{\alpha\beta} * V_{abc} \tag{5}$$

$$\begin{bmatrix} V_\alpha \\ V_\beta \end{bmatrix} = \begin{bmatrix} V_m \sin\theta \\ V_m \cos\theta \end{bmatrix} \tag{6}$$

The dq-transformation matrix is given as

$$T_{qd} = \begin{bmatrix} \sin\theta^* & \cos\theta^* \\ -\cos\theta^* & \sin\theta^* \end{bmatrix} \tag{7}$$

2.1. Response of SRF PLL during high frequency harmonic injection

The three phase input signal contains fundamental frequency of 50 Hz (1 p.u), with 33% of 3rd (0.33 p.u), 25% of 5th (0.25 p.u), 17% of 7th (0.17 p.u), 13% of 9th (0.13 p.u) and 8% of 11th (0.08 p.u) harmonics, shown in Fig. 2(a) and the corresponding actual and estimated phase is illustrated in Fig. 2(b). The estimated phase angle is tracked by synchronizing the voltage space vector along q-axis is shown in Fig. 2(c). It is shown that, SRF PLL system is sensitive to harmonics and the corresponding estimated phase contains second harmonic ripples (100 Hz). As result, the estimated frequency is not so accurate from the Fig. 2(d) with the presence of low frequency harmonics components in the PI controller output. Hence the Total Harmonic Distortion (THD) of the fundamental signal extracted by SRF PLL is found to be 6.51%.

3. Phase detection by DFT algorithm

This section reveals the generalized concept of DFT filtering for phase detection. As it is a recursive digital filter, the fundamental frequency/phase of the grid can be estimated accurately even with distorted input signal. Fig. 3 depicts the block diagram of conventional DFT filtering for phase detection. It consists of DFT, Moving average filter, proportional and integral (PI) controller and Numerically Controlled Oscillator (NCO).

3.1. DFT

Consider a time signal x(t) that is sampled at the rate of N * f to produce a time sequence of x(n) which contain the N data points

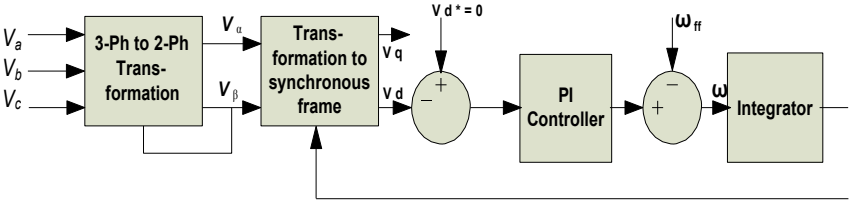

Fig. 1. Basic structure of SRF PLL system.

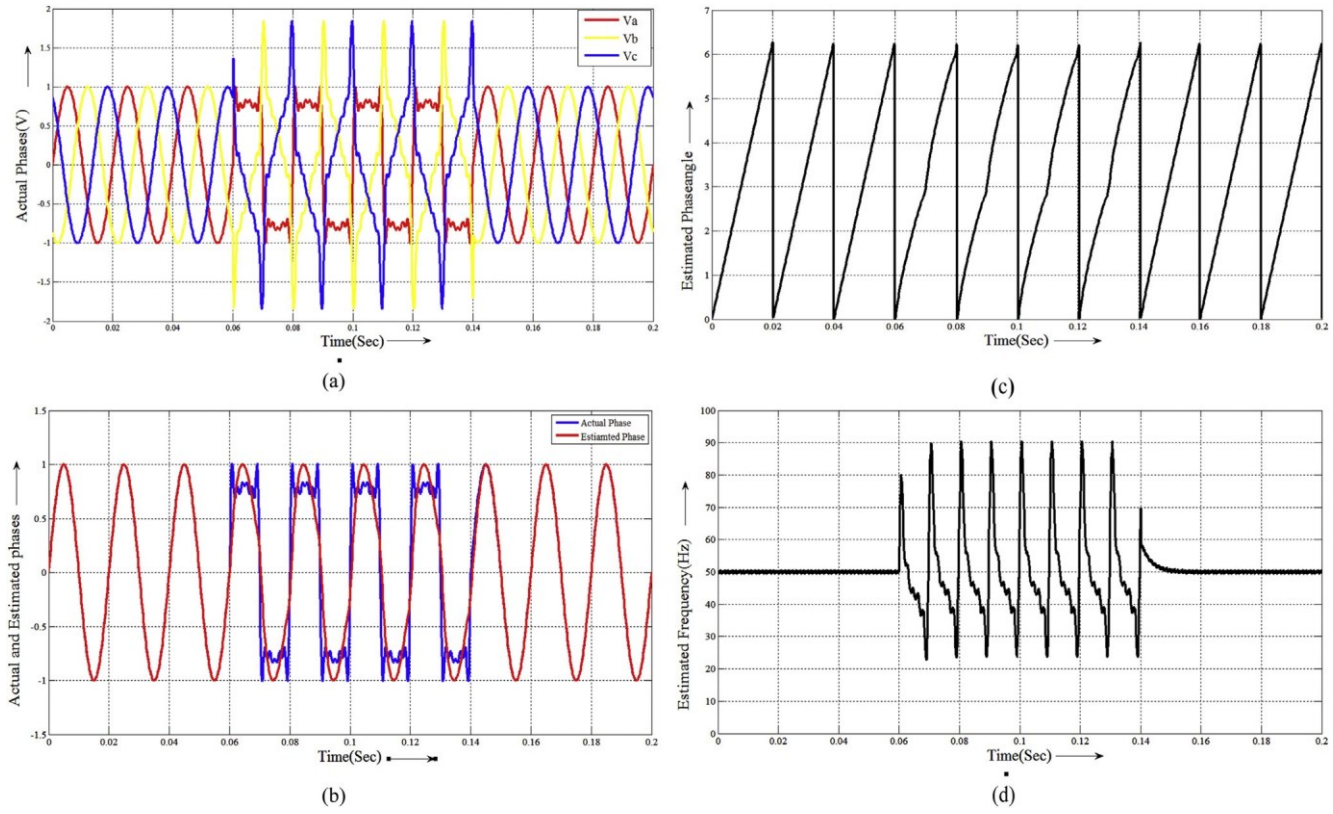

Fig. 2. Response of SRF PLL during high frequency harmonic injection. (a) Three phase grid voltage waveforms. (b) Actual and estimated phases. (c) Estimated phase angle. (d) Estimated fundamental frequency.

[9]. Where f is the fundamental signal frequency. The DFT produce the kth harmonics of x(n) at unit time delay and it can be written as

$$X_k\ n-1\ \ ¼ \sum_{n-N} x\ n\ e^{ð-j2pðn-1Þk=NÞ} \tag{8}$$

A new time sample of x(t) is taken and the DFT at the one time step later n becomes

$$X_k\ n\ ¼ \sum_{n-NÞ1} x\ n\ e^{ð-j2pðn-1Þk=NÞ} \tag{9}$$

Subtracting (8) from (9), we get

$$X_k\ n\ \ ¼ X_k\ n-1\ \ Þ\ x\ n\ \ -x\ n-N\ \ e^{ð-j2pkðn-1Þ=NÞ} \tag{10}$$

This equation is a recursive expression for the DFT of x(n).

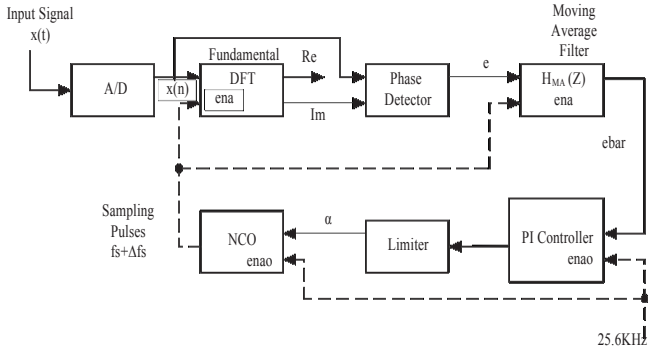

Fig. 3. Block diagram of DFT filtering for phase detection.

Take Z transform for Equation (3), we get

$$H\ Z\ \ ¼ \frac{X_k ðnÞ}{X ðnÞ} ¼ \frac{1-Z^{-N}}{1-Z^{-1}}\ e^{ðj2pðn-1Þk=NÞ} \tag{11}$$

The real part of recursive DFT is

$$Re½X_k ðnÞ] ¼ \frac{1-Z^{-N}\ x\ n}{1-Z^{-1}} \cos ð2pðn-1Þk=NÞ \tag{12}$$

The imaginary part of recursive DFT is

$$Im½X_k ðnÞ] ¼ \frac{1-Z^{-N}\ x\ n}{1-Z^{-1}}\ \ -\sin ð2pðn-1Þk=N \tag{13}$$

Based on Equations (12) and (13) the DFT structure is shown in Fig. 4.

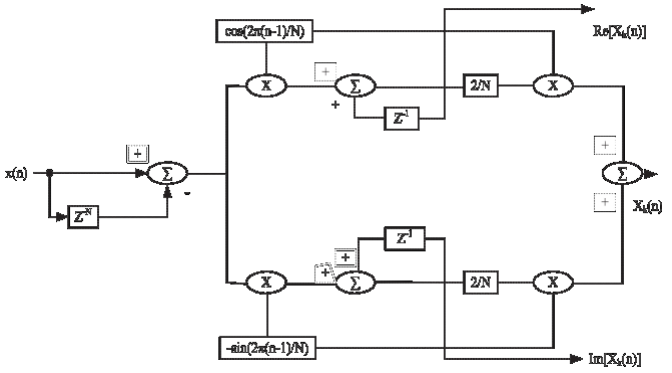

Fig. 4. Structure of DFT.

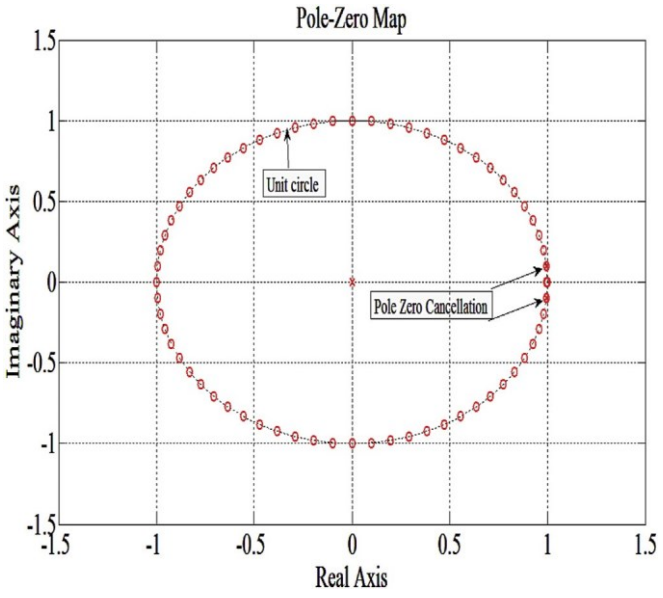

Fig. 5. Pole-zero plot for a DFT filter with N ¼ 64, k ¼ 1.

The inverse DFT of $x_k(n)$ is defined as

$$x_k(n) = G(k)\, X_k(n)\, e^{\delta j 2p\delta} \quad G(k) = \begin{cases} N^{-1} : k = 0; N \\ 2N^{-1} : \text{otherwise} \end{cases} \tag{14}$$

By taking Z transforms for Equations (3) and (7), the final simplified form of Z-transform of the DFT become

$$\frac{x_k(Z)}{X_k(Z)} = \frac{1}{N}\left[\frac{1 - Z^{-N}}{1 - e^{j2pk/N} Z^{-1}} + \frac{1 - Z^{-N}}{1 - e^{-j2pk/N} Z^{-1}}\right] \tag{15}$$

For fundamental frequency extraction by DFT, the 'k' value become one and therefore Equation (15) can be written as

$$\frac{x_1(Z)}{X_1(Z)} = \frac{1}{N}\left[\frac{1 - Z^{-N}}{1 - e^{j2p/N} Z^{-1}} + \frac{1 - Z^{-N}}{1 - e^{-j2p/N} Z^{-1}}\right] \tag{16}$$

From (16), the filter characteristics of DFT can be determined.

3.1.1. Frequency response of DFT filter

The frequency response of DFT filter defines the noise rejection capability and phase response of the system, and can be derived from Equation (16). Fig. 5 illustrates the pole-zero plot for DFT filtering. As one can be seen that, two poles are cancel with zeros and N − 2 zeros equidistantly spaced on the unit circle. As a consequence, the filter has a finite impulse response (FIR) equal to one time window period (1/f) and it leads to the DFT filter is unconditionally stable [8]. The corresponding frequency response of DFT filtering is illustrated in Fig. 6 with time window of 20 ms and 64 samples per time window. For low frequencies the magnitude envelope initially rolls off at 30 dB/decade but asymptotes to 20 dB/decade such that at 1 Hz the magnitude response is −53.5 dB. This characteristic shows that filter will attenuate the effect of sub harmonic in the line voltage. For frequency greater than the fundamental signal frequency (f) the harmonic rejection is clear, and the magnitude envelope rolls-off at 20 dB/decade up to the sampling frequency(f_s ¼ 3200 Hz) Therefore the DFT filter shows the band pass characteristics [13].

4. Improved SDFT algorithm for phase detection

Fig. 7 depicts the improved phase detection system using SDFT in order to track the frequency and phase of fundamental component of grid voltage. The proposed system consists of SDFT, Moving average filter, PI controller and Numerically Controlled Oscillator (NCO). This section describes the detailed analysis of proposed SDFT for phase detection.

4.1. SDFT

With reference to E. Jacobsen et al., in the proposed SDFT, the computation involves for N samples and the SDFT requires 4N real multiplication and 4N real addition, whereas DFT requires 2N real multiplication and 2N real additions. The computational complexity of each successive N-point output is O (N^2) for DFT,

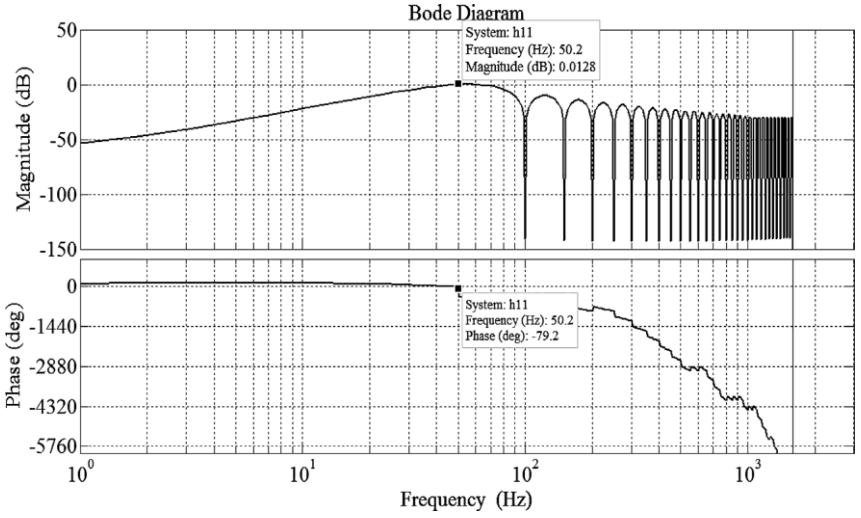

Fig. 6. Frequency response of the DFT filter, N ¼ 64, k ¼ 1.

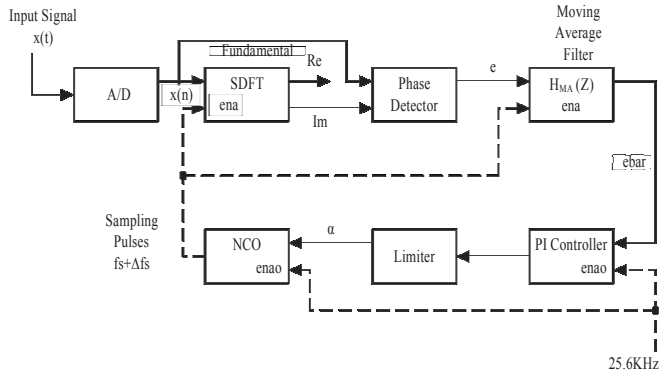

Fig. 7. Block diagram of novel SDFT based PLL.

O(Nlog 2N) for FFT and O(N) for SDFT. As a result, SDFT filtering is more efficient as it requires small number of operations to extract a single frequency component, thereby reducing computational complexity and simpler than DFT [10].

Moreover, SDFT is a versatile algorithm capable of extracting in phase and quadrature components of fundamental frequency from distorted grid voltages. In this work SDFT filter is designed for the signal with the fundamental frequency of f, window width N, and the sampling frequency f_s. If it is driven by another signal whose frequency is f þ Df, the sin and cosine output show a phase shift of Df which is proportional to Df_s. This property is highly useful for phase detection, which adjusts f_s to f_s þ Df_s making the use of Df. In addition to that, the proposed SDFT compute the N-point DFT for a single bin (k), centered at an angle θ_k ¼ 2pk/N rad, on the unit circle, which is corresponding to the cyclic frequency of kf_s/N Hz. The bin index k is 0 ::: k < N. However, for successful implementation of SDFT, the sampling frequency (f_s) should be equal to the nominal fundamental signal frequency (f) and window width N. Thus the SDFT phase detection is a real-time signal processing algorithm which is insensitive to harmonics distortion and robust against frequency and phase variations [8].

The N-point SDFT Equation [9] of x(n) for nth instant is

$$X_k(n) = X_k(n-1) - x(n-N) + x(n)\, e^{j2\pi k/N} \tag{17}$$

where x(n − N) is delay input sample and x(n) is current input sample.

The transfer function in the z-domain for the kth bin SDFT is

$$H(Z) = \frac{1 - Z^{-N}}{1 - e^{j2\pi k/N} Z^{-1}} \tag{18}$$

The factor $1 - Z^{-N}$ is a comb filter of the finite-impulse response (FIR). The real and imaginary component of $X_k(n)$ can be generated from resonator and comb filter. The structure of SDFT for kth bin is shown in Fig. 8. The real and imaginary component of H(Z) is given as;

$$\mathrm{Re}[H(Z)] = \frac{1 - Z^{-N}\cos 2\pi k/N - Z^{-1}}{1 - 2\cos 2\pi k/N\, Z^{-1} + Z^{-2}} \tag{19}$$

$$\mathrm{Im}[H(Z)] = \frac{1 - Z^{-N}\sin 2\pi k/N}{1 - 2\cos 2\pi k/N\, Z^{-1} + Z^{-2}} \tag{20}$$

In the phase detector, the exact cosine signal obtained from fundamental SDFT bin (k ¼ 1) is multiplied with the input signal to yield e. The output from the phase detector is given to moving average filter in order to reduce the phase margin. The output of the moving average filter is processed by a PI controller, which provides the control input for numerically controlled oscillator (NCO) with zero steady state error. Hence NCO generates the sampling pulses at required rate.

4.2. PI controller

In order to provide the steady dc input a to the NCO, even when the phase error tends to zero at steady state, a PI controller is combined with the phase detection circuit. Thus the transfer function of the controller in the frequency domain is

$$H_{PI}(Z) = K_p + \frac{K_p T_{enao}}{T_i\,(1 - Z^{-1})} \tag{21}$$

where K_p is the proportional gain, T_i integral time constant and T_{enao} is the enabling time, for the PI block. The enabling frequency f_{enao} ¼ $(1/T_{enao})$ was fixed at 25.6 kHz. The output of the PI controller is limited to ±1. And the Saturation limits are allowed to prevent overflow of the integrator registers, which can incidentally limits the control input a applied to the NCO.

4.3. Frequency response characteristics

The frequency response characteristic of SDFT filtering defines the noise rejection capability and phase response of the system, and can be calculated from the Z-transform of the Equation (18). From that, pole-zero plot for SDFT filtering is plotted and is given in Fig. 9. And it reveals that, two poles are canceling with zeros and N − 2 zeros equidistantly spaced on the unit circle. The extraction of single frequency component produces two poles that cancel with zeros. The poles are located on the unit circle and therefore the

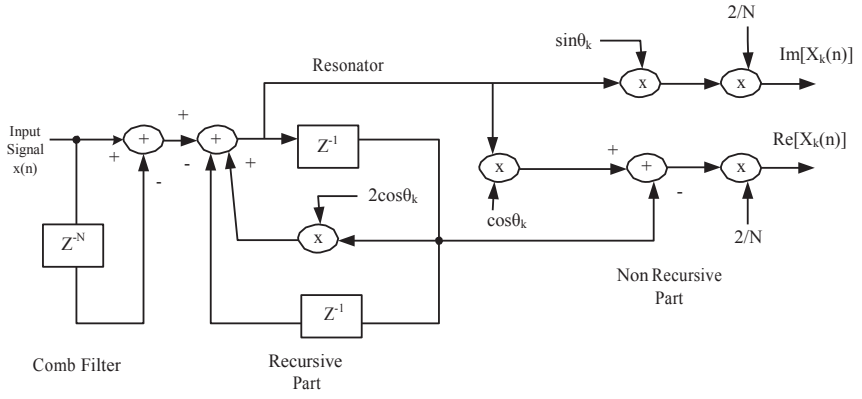

Fig. 8. SDFT structure.

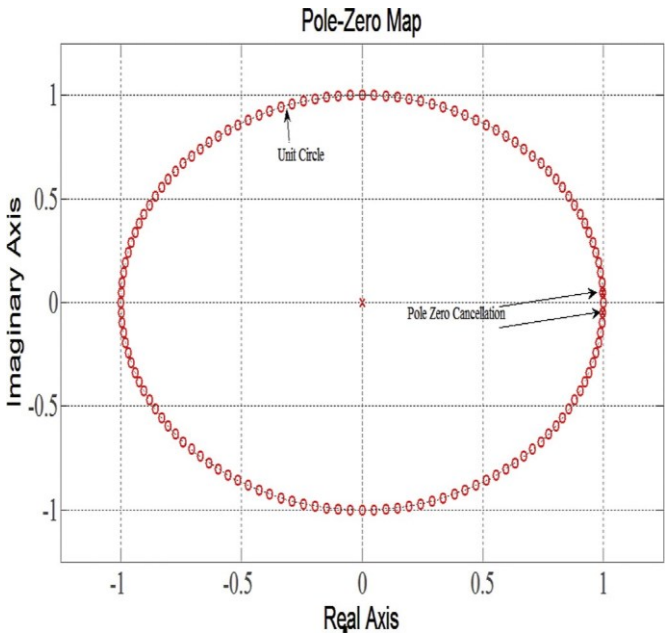

Fig. 9. Pole-zero plot for a SDFT filter with N ¼ 128, k ¼ 1.

SDFT filter is stable [11]. The frequency characteristics of a single-bin sliding filter for N ¼ 128 and k ¼ 1 is illustrated in Fig. 10. It states that, the corresponding to the value of 'k', it allows the fundamental frequency component of grid voltage with rejection of all sub and higher order harmonic components. So it reveals neither passband nor stopband characteristics of the filter, but they adequate for coherent sampled signals [11].

5. Results and discussion

In order to analyze the proposed study, simulations tests have been carried out in the MATLAB-Simulink environment and the following parameters are considered for the study.

Input voltage U ¼ 230 V(rms), f ¼ 50 Hz, N ¼ 128, f_{enao} ¼ 25.6 kHz, K_p ¼ 0.01 and K_i ¼ 0.0026.

The abnormal conditions namely; high frequency harmonic injection, frequency variation and phase variation of grid voltages are examined for accurate phase detection in this study using SDFT algorithm.

5.1. Response of DFT filtering

5.1.1. High frequency harmonic injection

The input signal contains fundamental frequency of 50 Hz, with 33% of 3rd, 25% of 5th, 17% of 7th, 13% of 9th and 8% of 11th harmonics which is shown in Fig. 11(a) according to Equation. (22) as given below.

$$x(t) = 325{:}27\sin(\omega t) + 107{:}34\sin(3\omega t) + 81{:}32\sin(5\omega t) + 55{:}30\sin(7\omega t) + 42{:}28\sin(9\omega t) + 26{:}02\sin(11\omega t) \quad (22)$$

This input signal is given to conventional DFT filtering the real and orthogonal signals are extracted and the corresponding obtained results are shown in Fig. 11(b).The actual and estimated phases and phase angles are extracted at accurate sampling rate by using NCO as shown in Figs. 11(c) and Fig. 13(d) respectively. Total Harmonic Distortion (THD) of harmonic contented input signal is 47.29% and the fundamental signal extracted by DFT with the THD of extracted signal is 3.28% which is shown in Fig. 11(e).

5.2. Response of SDFT filtering

This section describes the superior performance of SDFT filtering for phase detection during adverse situation of grid such as high frequency harmonic injection, Frequency deviation and Phase variation etc.

5.2.1. Harmonic injection

By injecting the same input signal as shown in Fig. 12(a) to SDFT filtering, the fundamental frequency component is accurately extracted as compared to DFT filtering. On the other hand, the proposed recursive SDFT filtering is less sensitive to harmonics and grid parameter variations. The corresponding estimated real and orthogonal signals are shown in Fig. 14(a). The actual and estimated phases and phase angles are extracted at accurate sampling rate by using NCO as shown in Fig. 12(b) and (c) respectively. As a result, the THD of grid voltage is reduced to 1.65% with more fundamental component as compared to DFT filtering which is depicted in Fig. 12(d).

5.2.2. Frequency deviation

In order to test the transient response of proposed SDFT filtering system, same frequency variation is considered which is depicted in Fig. 13(a) with the frequency of the input signal changed from

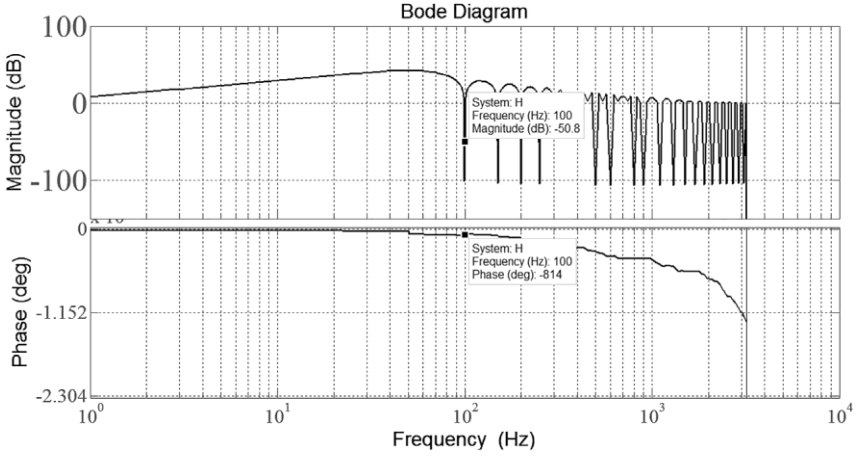

Fig. 10. Frequency response of the SDFT filter, N ¼ 128.

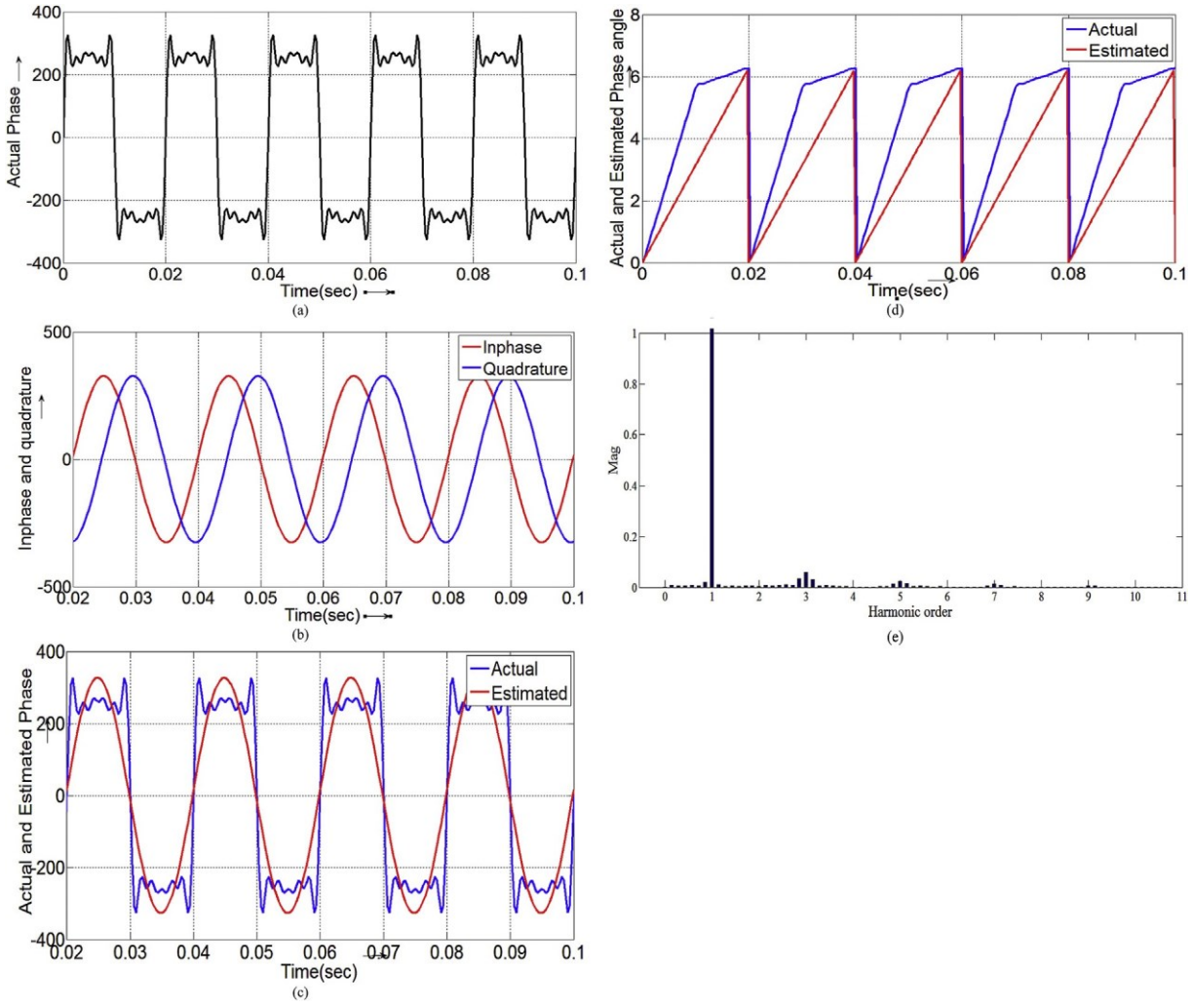

Fig. 11. Response of DFT filtering during harmonic injection. (a) Input signal with harmonic injection. (b) Inphase and quadrature components. (c) Response of actual and estimated phases. (d) Actual and estimated phase angle. (e) THD of grid voltages.

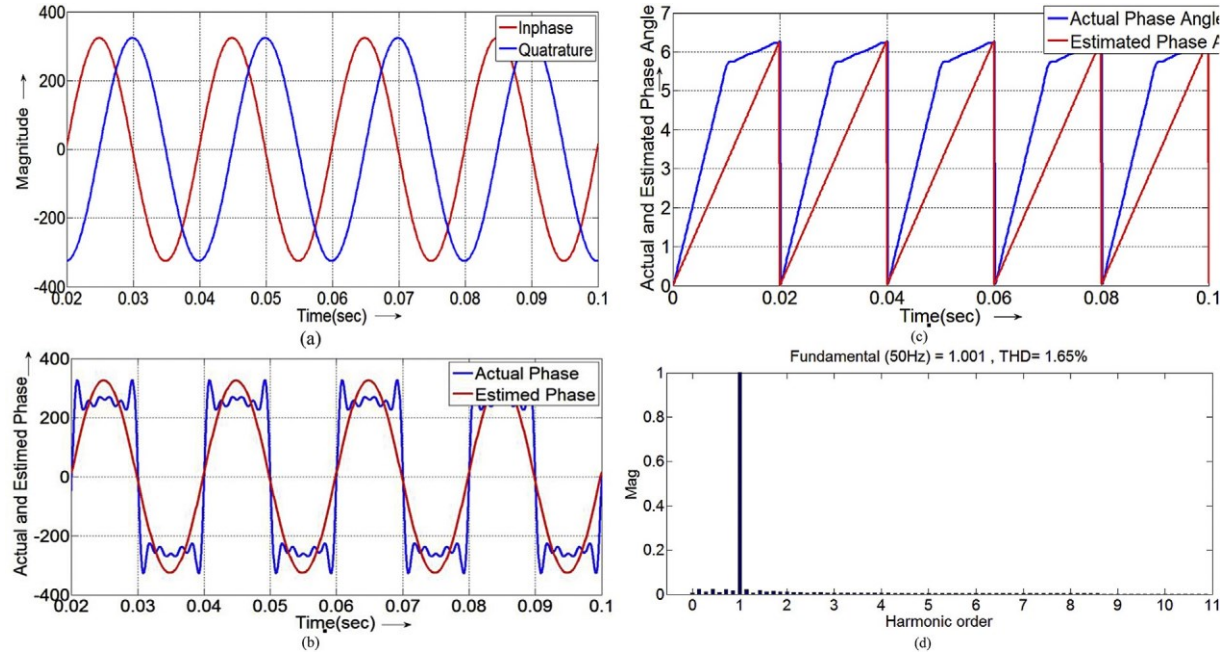

Fig. 12. Response of SDFT filtering during harmonic injection. (a) Inphase and quadrature components. (b) Response of actual and estimated phases. (c) Actual and estimated phase angle. (d) THD of grid voltages.

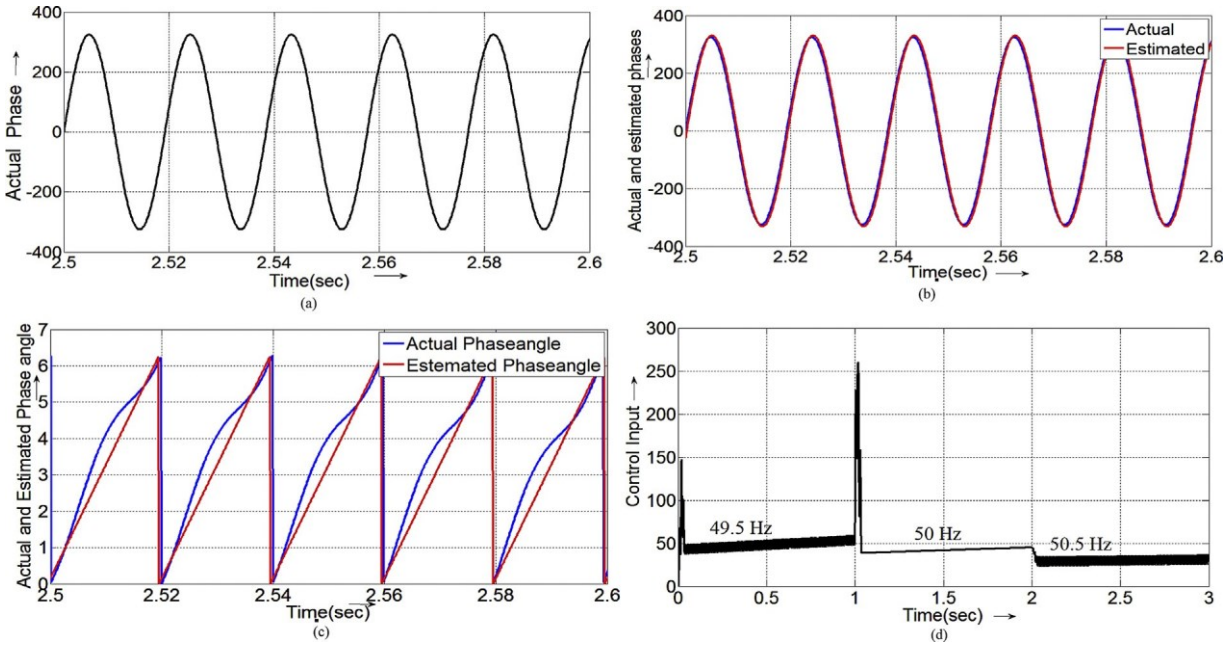

Fig. 13. Response of SDFT filtering during frequency deviation. (a) Input signal with frequency variation (zoomed view). (b) Actual and estimated phases. (c) Actual and estimated phase angle. (d) Transient response of DFT filtering.

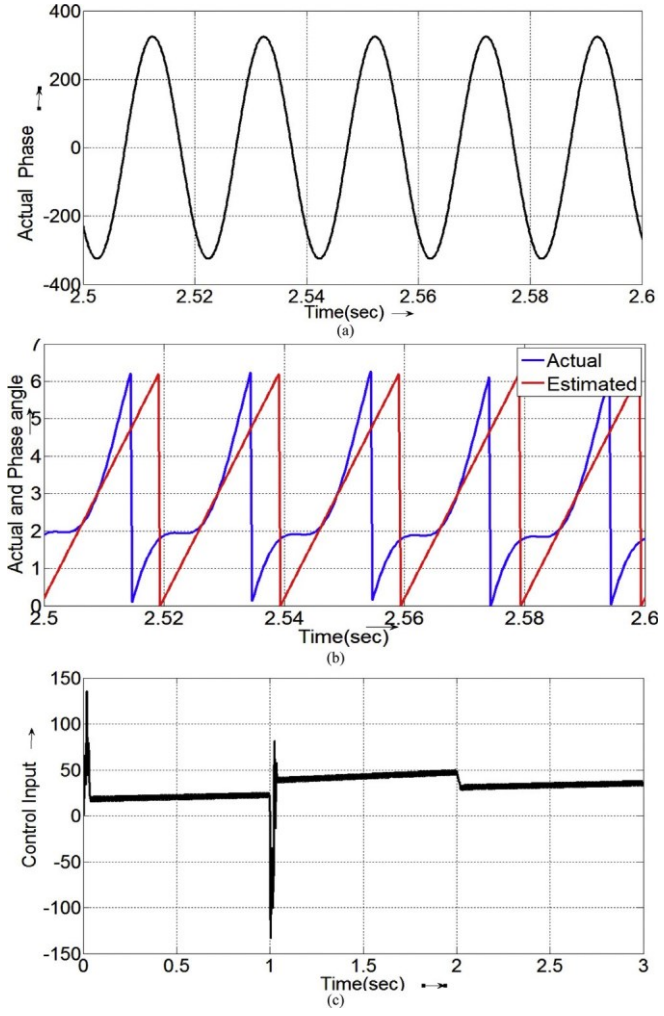

Fig. 14. Response of SDFT filtering during phase variation (a) Input voltage waveform (input voltage þ1.57 rad (zoomed view). (b) Actual and estimated phase angles. (c) Control input for ±1.57 rad step change in phase in 50 Hz.

49.5 Hz to 50 Hz at 1 s and from 50 Hz to 50.5 Hz at 2 s. The actual and estimated phases and phase angles are extracted at sampling rate by using NCO as shown in Fig. 13(b) and (c) respectively. As an evidence of Fig. 13(d), the PI controller output settles at the new value of a from 52 to 48 at 1sec when frequency changes from 49.5 Hz to 50 Hz as shown in Fig. 13(d). It is observed that, the proposed DFT filtering can be able to accurately estimate the phase of the fundamental signal during frequency variations. Therefore, the precise detection of phase angle is realized by the proposed SDFT filtering. In exacting, the transient response of sliding DFT filtering is faster than DFT filtering scheme.

5.2.3. Phase variation

The transient performance of the proposed SDFT filtering during phase variation is also tested for better understanding. The phase of the input signal set to þ1.57 rad (U_m * sin(ut þ (p/2)) at 0 s, −1.57 rad (U_m * sin(ut − (p/2)) at 1 s and þ1.57 rad (U_m * sin(ut þ (p/2)) at 2 s the zoomed view as shown in Fig. 14(a). The actual and estimated phases are extracted by SDFT using enabling pulse applied by NCO as shown in Fig. 14(b). The PI controller output settles at the new value of a from 30 to 48 when phase changes to −1.57 rad at 1 s as shown in Fig. 14(c). Therefore the transient response of SDFT is faster than DFT filtering scheme. In addition to that, the acquisition of fundamental signal is faster than DFT filtering scheme [12].

6. Conclusions

This work proposes and alternative method of phase detection based on SDFT algorithm for grid synchronization of distributed generation system. From the proposed study it was observed that, SDFT phase detection system is more efficient as it requires small number of operations to extract a single frequency component, thereby reducing computational complexity and simpler than DFT. Moreover, SDFT can enable to extract the fundamental frequency of the phase accurately during adverse condition of the grid. Thus the proposed phase detection system that in addition to detecting the grid phase angle and frequency can detect current harmonics and extract the active/reactive current component for power quality

purposes. Therefore, the immediate advantages of the proposed PLL are: frequency adaptability, high degree of immunity to disturbances and harmonics, and structural robustness. Moreover, the proposed synchronization scheme can further be used for grid measuring, monitoring and processing of the grid signal.

References

[1] F. Iov, R. Teodorescu, Blaabjerg, B. Andersen, J. Birk, J. Miranda, Grid code compliance of grid-side converter in wind turbine systems, in: Proc. of 37th IEEE Power Electronics Specialists Conference, 2006, pp. 1e6. PESC '06.

[2] Francisco D. Freijedo, Jesus Doval-Gandoy, Oscar Lopez, Carlos Martinez-Penalver, Alejandro G. Yepes, Pablo Fernandez-Comesana, Andres Nogueiras, Jano Malvar, Jorge Marcos, Alfonso Lago, Grid-synchronization methods for power converters, in: Proc. of IEEE 35th Industrial Electronics Society Annual Conference. IECON '09, 2009, pp. 522e529.

[3] L.N. Arruda, S.M. Silva, B.J.C. Filho, PLL structures for utility connected systems, in: Industry Applications Conference, 2001. Thirty-sixth IAS Annual Meeting. Conference Record of the 2001 IEEE, Oct. 2001, pp. 2655e2660.

[4] R.I. Bojoi, G. Griva, V. Bostan, M. Guerriero, F. Farina, F. Profumo, Current control strategy for power conditioners using sinusoidal signal integrators in synchronous reference frame, IEEE Trans. Power Electron. 20 (6) (Nov. 2005) 1402e1412.

[5] R. Weidenbrug, F.P. Dawson, R. Bonert, New synchronization method for thyristor power converters to weak AC systems, IEEE Trans. Ind. Electron. 40 (05) (1993) 505e511.

[6] D. Yazdani, A. Bakhshai, G. Joos, M. Mojiri, A nonlinear adaptive synchronization technique for single-phase grid-connected converters, in: IEEE PESC 2008 Power Electronics Specialists Conference, 2008, 2008, pp. 4076e4079.

[7] Brendan Peter McGrath, James Jim H. Galloway, Power converter line synchronization using a discrete Fourier transform (DFT) based on a variable sample rate, IEEE Trans. Power Electron. 20 (04) (2005) 877e883.

[8] P. Sumathi, P.A. Janakiraman, Integrated phase-locking scheme for SDFT based harmonic analysis of periodic signal, IEEE Trans. Circuit Syst. II 55 (1) (Jan 2008) 51e55.

[9] S.K. Panda, B. Chitti Babu, Improved phase detection technique for grid synchronization of DG systems during grid abnormalities, in: Proc. IEEE Students' Conference on Engineering and Systems (SCES), April 2013, pp. 01e06.

[10] E. Jacobsen, R. Lyons, The sliding DFT, IEEE Signal Process. Mag. 20 (2) (Mar.2003) 74e80.

[11] R. Lyons, A. Bell, The Swiss army knife of digital networks, IEEE Signal Process. Mag. 21 (3) (May 2004) 90e100.

[12] E. Jacobsen, R. Lyons, An updated the sliding DFT, IEEE Signal Process. Mag. 21 (1) (Jan.2004) 110e111.

[13] C.S. Tuner, Recursive discrete-time sinusoidal oscillator, IEEE Signal Process. Mag. 20 (3) (May 2003) 103e111 exist.